Short-wavelength turbulence in the solar wind: Linear theory of whistler and kinetic Alfvén fluctuations

S. Peter Gary

Los Alamos National Laboratory, Los Alamos, New Mexico

Charles W. Smith

University of New Hampshire, Durham, New Hampshire

S. P. Gary, Los Alamos National Laboratory, M.S. D466, Los Alamos, NM 87545 (pgary@lanl.gov)

C. W. Smith, University of New Hampshire, Durham, New Hampshire 03824 (chuck@briaxa.sr.unh.edu)

Abstract. There is a debate as to the identity of the fluctuations which constitute the relatively high-frequency plasma turbulence observed in the solar wind. One school holds that these modes are kinetic Alfvén waves, whereas another opinion is that they are whistler modes. Here linear kinetic theory for electromagnetic fluctuations in homogeneous, collisionless, magnetized plasmas is used to compute two dimensionless transport ratios, the electron compressibility C_e and the magnetic compressibility $C_{\|}$ for these two modes. The former is a measure of the amplitude of density fluctuations, and the latter indicates the relative energy in magnetic fluctuations in the component parallel to the background magnetic field $\mathbf{B}_o$. For $\beta_e << 1$, $[C_{\|}]_{Alfven} << [C_{\|}]_{whistler}$, and the latter quantity is of order 0.5 at whistler propagation strongly oblique to $\mathbf{B}_o$. Such values of $C_{\|}$ are sometimes measured at relatively high frequencies and $\beta_e << 1$ in the solar wind; thus it is concluded that such observations correspond to whistler mode turbulence. But the overall body of solar wind observations indicates that kinetic Alfvén fluctuations also contribute to relatively high frequency solar wind turbulence.

1. Introduction

Measurements of solar wind turbulence from single spacecraft consistently show that, in the range of observed frequencies 10^{-4} Hz $\lesssim f' \lesssim$ 0.2 Hz, magnetic fluctuation energy spectra have a power-law dependence:

$$\frac{|\delta \mathbf{B}(f')|^2}{8\pi} \sim (f')^{-\alpha}$$

The observations in this frequency regime, which is termed the inertial range, indicate $\alpha \simeq 5/3$ with relatively small variations about this value [*Horbury et al.*, 2005; *Smith et al.*, 2006a].

Further solar wind observations have examined inertial range turbulence spectra as functions of wavenumbers $k_\parallel$ and $k_\perp$, where the symbols $\parallel$ and $\perp$ denote directions parallel and perpendicular, respectively, to the background magnetic field $\mathbf{B}_o = \hat{\mathbf{z}} B_o$. A wavevector anisotropy is generally observed; that is, for a given k magnetic fluctuation energy is stronger at quasi-perpendicular propagation ($k_\perp >> k_\parallel$) than it is at quasi-parallel propagation ($k_\perp << k_\parallel$) [*Matthaeus et al.*, 1990; *Horbury et al.*, 2005; *Dasso et al.*, 2005]. Both parallel and perpendicular reduced power spectra are observed to exhibit power-law dependence on wavenumber, that is,

$$\frac{|\delta \mathbf{B}(k_\parallel)|^2}{B_o^2} \equiv \frac{\sum_{k_\perp} |\delta \mathbf{B}(\mathbf{k})|^2}{B_o^2} \sim k_\parallel^{-\alpha_\parallel}$$

and

$$\frac{|\delta \mathbf{B}(k_\perp)|^2}{B_o^2} \equiv \frac{\sum_{k_\parallel} |\delta \mathbf{B}(\mathbf{k})|^2}{B_o^2} \sim k_\perp^{-\alpha_\perp}$$

Solar wind measurements generally yield $\alpha_\perp \simeq 1.6$ and a similar value for $\alpha_\parallel$ [*Tessein et al.*, 2009, and references therein]. However, some observations show a steeping of spectra at quasi-parallel propagation with $\alpha_\parallel \simeq 2.0$ [*Horbury et al.*, 2008; *Podesta*, 2009].

Magnetohydrodynamic (MHD) simulations of inertial range turbulence also demonstrate a power law dependence of magnetic energy density on wavenumber, with $3/2 \lesssim \alpha \lesssim 5/3$ [*Müller and Grappin*, 2005] and a wavevector anisotropy in the same sense as in the solar wind [*Oughton and Matthaeus*, 2005]. MHD computations further demonstrate that the sense of fluctuation energy transfer in plasma turbulence is usually via a forward cascade; that is, energy is injected at very long wavelengths, and then is transported via wave-wave interactions down through successively shorter wavelengths to eventual dissipation at some sufficiently large k.

Inertial range spectra are observed to change near 0.2 Hz $\lesssim f' \lesssim$ 0.5 Hz, where, following a distinct breakpoint, higher frequencies correspond to steeper power-law spectra with a broader range of α values ($2.0 \lesssim \alpha \lesssim 4$) [*Leamon et al.*, 1998; *Smith et al.*, 2006a; *Alexandrova et al.*, 2008; *Hamilton et al.*, 2008]. Recently *Sahraoui et al.* [2009] and *Alexandrova et al.* [2009] used solar wind magnetic field measurements from Cluster spacecraft to show that magnetic fluctuation spectra at frequencies above the inertial range breakpoint can consist of two distinct regimes with successively steeper slopes as functions of f'. *Sahraoui et al.* [2009] fit their observations of an intermediate-frequency range over 0.4 Hz $\lesssim -f' \lesssim$ 35 Hz as a power law with $\alpha \simeq 2.5$ and report a similar frequency power-law fit with $\alpha \simeq 4.0$ to observations on a high-frequency regime over 35 Hz $\lesssim f' \lesssim$ 100 Hz. *Alexandrova et al.* [2009] find a power-law fit with $\alpha \simeq 2.8$ on their intermediate-frequency range over 1 Hz $\lesssim f' \lesssim$ 10 Hz, but show that an exponentially decreasing spectrum provides a better fit to their high-frequency measurements at 10 Hz $\lesssim f'$. *Sahraoui et al.* [2009] interpret the intermediate-frequency regime as corresponding to a dispersion cascade, and both papers attribute the high-frequency regime as due

to the consequences of wave-particle dissipation. Some earlier papers applied the term "dissipation range" to the intermediate frequency regime, by analogy with steep high-frequency spectra in fluid turbulence. However, in light of these new observational results, we here label intermediate frequency spectra as the "dispersion range" after *Stawicki et al.* [2001], and apply the term "dissipation range" only to the highest frequency domain.

The physics of plasma turbulence at and beyond the inertial range breakpoint is not well understood. Some observations indicate that this breakpoint wavenumber scales as the inverse proton inertial length; that is, $kc/\omega_p \sim 1$ where ω_p is the proton plasma frequency [*Leamon et al.*, 2000; *Smith et al.*, 2001; *Alexandrova et al.*, 2008]. Other experimental interpretations associate this feature with the proton gyroradius, i.e., $kv_p/\Omega_p \sim 1$ where v_p is the proton thermal speed and Ω_p is the proton cyclotron frequency [*Bale et al.*, 2005; *Sahraoui et al.*, 2009]. And the *Markovskii et al.* [2008] analysis of spacecraft measurements suggests a nonlinear scaling for the inertial breakpoint wavenumber. Two fundamental, unanswered questions concerning turbulence at and above the inertial range breakpoint are: first, what dissipation mechanisms are acting here and and, second, what are the dispersion properties, that is, what are the principal constitutent modes?

This manuscript describes research toward answering the second of these questions. First, however, it is necessary to define our terms. Linear kinetic theory for stable, homogeneous, collisionless plasmas yields three types of normal modes at and below Ω_p. The predominantly electrostatic ion acoustic mode (also called the "slow" mode) is strongly damped unless $T_e >> T_p$; as this condition arises infrequently in the solar wind, we do not include this mode as a contributor to the turbulence considered here. At $\mathbf{k} \times \mathbf{B}_o = 0$ and $\omega_r < \Omega_p$, there are two incompressibile electromagnetic modes: left-hand polarized

Alfven-cyclotron waves and right-hand polarized magnetosonic fluctuations. As $\mathbf{k}$ becomes relatively oblique to $\mathbf{B}_o$, both modes develop a non-zero magnetic compressibility, which we define as

$$C_{\parallel}(\mathbf{k}) \equiv \frac{|\delta B_{\parallel}(\mathbf{k})|^2}{|\delta \mathbf{B}(\mathbf{k})|^2} \quad . \tag{1}$$

At quasi-perpendicular propagation the modes which evolve from the Alfvén-cyclotron branch are known as kinetic Alfvén waves; here we also distinguish the quasi-parallel magnetosonic and quasi-perpendicular magnetosonic modes. In contrast to the Alfvénic modes, magnetosonic modes may propagate to frequencies above Ω_p; at $\Omega_p << \omega_r$ they are called whistler modes. We also distinguish between relatively incompressible quasi-parallel whistlers and quasi-perpendicular whistlers with substantial magnetic compressibility [*Saito et al.*, 2008].

There are two distinct scenarios for the forward cascade of collisionless plasma turbulence from long wavelengths through the inertial range breakpoint and into the dispersion regime. In one scenario [*Howes*, 2008; *Schekochihin et al.*, 2009], compressive modes are regarded as damped in the collisionless inertial range, but long-wavelength Alfvénic turbulence cascades down to the scale of the ion gyroradius, a_i, where the fluctuations are subject to ion Landau damping. Therefore in this scenario the spectral breakpoint corresponds to $k_{\perp} a_i \sim 1$, where a_i is the thermal ion cyclotron radius; such a breakpoint has been demonstrated in the gyrokinetic simulations of *Howes et al.* [2008a] (See also the comments of *Matthaeus et al.* [2008] and the reply of *Howes et al.* [2008b].), as well as in Hall MHD computations [*Ghosh et al.*, 1996; *Galtier and Buchlin*, 2007; *Shaikh and Shukla*, 2009]. The remaining fluctuation energy continues to cascade to shorter wavelengths as kinetic Alfvén waves at quasi-perpendicular propagation and at real frequencies

$\omega_r < \Omega_p$, the proton cyclotron frequency [*Leamon et al.*, 1998; *Bale et al.*, 2005; *Sahraoui et al.*, 2009]. These fluctuations finally are completely damped via the electron Landau resonance at wavelengths of the order of the electron gyroradius.

In the second scenario both the Alfvénic modes and the magnetosonic modes are lightly damped at $\beta_p \lesssim 1$ and $kc/\omega_p \lesssim 1$, and both contribute to the inertial range cascade. This two-mode cascade preferentially transfers fluctuation energy to quasi-perpendicular propagation; Landau damping of kinetic Alfvén waves increases as $k_\perp^2$ [*Gary and Borovsky*, 2004, 2008], quenching such modes so that they do not contribute to dispersion range spectra except at propagtion angles extremely close to perpendicular. Left-hand polarized Alfvén-cyclotron fluctuations at quasi-parallel propagation are subject to proton cyclotron damping at $k_\parallel c/\omega_p \sim 1$, and clearly do not contribute to dispersion range spectra. As quasi-perpendicular magnetosonic modes approach $k_\perp c/\omega_p \sim 1$, they break up into Bernstein modes near the first few harmonics of Ω_p; it is not known how these frequency-structured modes contribute to the turbulent cascade. But for $\beta_p \lesssim 1$, quasi-parallel magnetosonic modes are not damped at $k_\parallel c/\omega_p \simeq 1$ [*Stawicki et al.*, 2001]; although their cascade is weaker than at quasi-perpendicular propagation, it is non-negligible and a reduced amplitude of right-hand polarized fluctuations persist to become whistler turbulence at $k_\parallel c/\omega_p > 1$ [*Goldstein et al.*, 1994]. The conditions for onset of Alfvén-cyclotron damping and whistler dispersion imply that $k_\parallel c/\omega_p \simeq 1$ is the breakpoint condition in this scenario.

Continuing with the second scenario, the forward cascade of lightly damped whistlers at $\Omega_p < \omega_r$ has been demonstrated by electron magnetohydrodynamic (EMHD) simulations in both two dimensions [*Biskamp et al.*, 1996; *Dastgeer et al.*, 2000; *Wareing and*

Hollerbach, 2009] and three dimensions [*Biskamp et al.*, 1999; *Cho and Lazarian*, 2004] as well as by the two-dimensional particle-in-cell (PIC) simulations of *Gary et al.* [2008] and *Saito et al.* [2008]. These computations show that the whistler cascade leads to reduced spectra that are steeper functions of wavenumber than inertial range spectra, but that the fluctuation intensity is, like that of the inertial range, stronger at quasi-perpendicular than at quasi-parallel propagation. The PIC simulations also indicate that dissipation of whistler turbulence can be due to both the electron cyclotron resonance at $k_{\|}c/\omega_e \simeq 1$ and the electron Landau resonance at $k_{\perp}c/\omega_e \sim 1$. So, in this scenario, it is the whistler component which cascades to successively shorter wavelengths and which is the primary constituent dispersion range spectra. Such modes are not easily measured by the DC magnetometers which yield inertial range spectra in the interplanetary medium, but spacecraft instruments designed to observe higher frequency magnetic fluctuations have demonstrated the existence of turbulent-like whistler spectra in the solar wind [*Beinroth and Neubauer*, 1981; *Lengyel-Frey et al.*, 1996].

We denote the jth species plasma frequency as $\omega_j \equiv \sqrt{4\pi n_j e_j^2/m_j}$, the jth species cyclotron frequency as $\Omega_j \equiv e_j B_o/m_j c$, and $\beta_{\|j} \equiv 8\pi n_j k_B T_{\|j}/B_o^2$. Solutions to the linear dispersion equation are in terms of a wavevector $\mathbf{k}$ with real components and a complex frequency $\omega = \omega_r + i\gamma$. We define θ, the angle of mode propagation, by $\mathbf{k} \cdot \mathbf{B}_o = kB_o \cos(\theta)$, and assume $\mathbf{B}_o = \tilde{\mathbf{z}} B_o$ as well as $\mathbf{k} = \hat{\mathbf{y}} k_y + \hat{\mathbf{z}} k_z$. We consider an electron-proton plasma where subscript e denotes electrons and p stands for protons. In such a plasma the Alfvén speed is $v_A \equiv B_o/\sqrt{4\pi n_e m_p}$.

Section 2 of this manuscript describes linear theory calculations for kinetic Alfvén waves and whistler fluctuations at quasi-perpendicular propagation. We define the magnetic

compressibility via Equation (1), the out-of-plane magnetic energy ratio as

$$C_{\perp\perp}(\mathbf{k}) \equiv \frac{|\delta B_x(\mathbf{k})|^2}{|\delta \mathbf{B}(\mathbf{k})|^2} \quad , \tag{2}$$

and the compressibility of the jth plasma species as

$$C_j(\mathbf{k}) \equiv \frac{|\delta n(\mathbf{k})|^2}{n_o^2} \frac{B_o^2}{|\delta \mathbf{B}(\mathbf{k})|^2} \tag{3}$$

[*Gary*, 1993]. For all parameters considered here, $C_p \simeq C_e$, so we show results only for the electron compressibility.

Short-wavelength magnetic fluctuations in the solar wind have relatively small amplitudes, i.e. $|\delta B|^2 << B_o^2$, and so **under the assumption of weak wave-wave interactions, we may describe their** dispersion and damping by linear kinetic theory. Recent PIC simulations [*Saito et al.*, 2008] have shown good agreement between the predictions of linear theory and the simulated values of magnetic fluctuation ratios such as the magnetic compressibility, demonstrating that **this** approximation may indeed be valid for small-amplitude whistlers. Thus in the Conclusions section of this manuscript we argue that magnetic compressibilities calculated from linear theory may be used to help discern between whistler and kinetic Alfvén contributions to dispersion range turbulence under various conditions in the solar wind.

2. Linear theory

The linear kinetic theory results presented here are derived from a model of a homogeneous, isotropic, collisionless plasma with uniform $\mathbf{B}_o$. We further assume an electron-proton plasma in which the velocity distributions of both species are Maxwellian. We use numerical solutions of the full linear dispersion equation for arbitrary directions of propagation [*Gary*, 1993], making no approximations with respect to the smallness of any

plasma parameter, frequency, or wavevector component. We choose $T_e = T_p$ and $\beta_e = 0.10$ unless otherwise stated. Note that the wavenumber scales of the figures showing kinetic Alfvén wave theory results can be converted to the wavenumber scales of the whistler figures via the relation $k_\perp c/\omega_e = \sqrt{m_e/m_p}\ k_\perp c/\omega_p$.

Figure 1 illustrates the dispersion and damping of whistler fluctuations at three oblique angles of propagation, whereas Figure 2 shows the same properties for kinetic Alfvén fluctuations also at three oblique values of θ. Whistler dispersion at $\omega_p/c < k << \omega_e/c$ shows the parabolic dependence on wavenumber predicted by cold plasma theory:

$$\frac{\omega_r}{|\Omega_e|} \simeq \frac{k k_\parallel c^2}{\omega_e^2}$$

As kc/ω_e approaches unity, the electron cyclotron resonance asserts itself, providing not only a constraint on the real frequency $\omega_r < |\Omega_e|$, but also causing the rapid onset of cyclotron damping. Kinetic Alfvén fluctuations depart from the long-wavelength relation $\omega_r = k_\parallel v_A$ as $kc/\omega_p \gtrsim 1$; there is again the suggestion of a parabolic dependence of real frequency on wavenumber, but in this case the proton cyclotron resonance provides the upper bound $\omega_r \lesssim \Omega_p$ and leads to the rapid onset of cyclotron damping at $k_\parallel c/\omega_p \gtrsim 1$ [*Gary and Borovsky*, 2004]. If $k_\parallel c/\omega_p < 1$, there is a more gradual increase of electron Landau damping with increasing $k_\perp c/\omega_p$.

Figures 1 and 2 further show that, over $\omega_p/c < k \lesssim \omega_e/c$, the whistler is lightly damped over a broad range of quasi-perpendicular angles, $60^o < \theta < 90^o$, whereas the kinetic Alfvén fluctuations at such wavenumbers are lightly damped only for a very narrow cone of propagation, i.e., $89^o < \theta < 90^o$. Sample calculations not shown here demonstrate that the same result holds at larger values of β_e as well.

Fig. 3b of *Saito et al.* [2008] plots the whistler damping rate as a function of θ for fixed dimensionless wavenumber and $k_{||}c/\omega_e < 1$. The result that $|\gamma(\theta)|$ has a maximum at $\theta \simeq 60^o$ implies that there are two channels for the possible cascade of weakly damped whistler modes: one at quasi-parallel propagation, and another at quasi-perpendicular propagation.

Figure 3 plots the magnetic and electron compressibilities for the three whistler cases illustrated in Figure 1, whereas Figure 4 illustrates the same quantities for the kinetic Alfvén cases of Figure 2. The dispersion range turbulence observed in the solar wind likely corresponds to $1 << k_\perp c/\omega_p \lessapprox \sqrt{m_p/m_e}$. In this regime, quasi-perpendicular whistler fluctuations at $\beta_e \simeq 0.10$ have $C_{||} \sim 0.5$ whereas kinetic Alfvén fluctuations at the same β_e display $C_{||} << 1$. So it is clear that, at $\beta_e << 1$,

$$[C_{||}]_{Alfven} << [C_{||}]_{whistler} \tag{4}$$

At sufficiently large perpendicular wavenumbers and $\beta_e = 0.10$, comparison of the two figures shows that the electron compressibility has the opposite relationship:

$$[C_e]_{Alfven} >> [C_e]_{whistler} \tag{5}$$

Figures 5 and 6 show $C_{||}(k_\perp)$ and $C_e(k_\perp)$ for the quasi-perpendicular whistler and kinetic Alfvén modes, respectively, at several values of β_e. These figures show that, for the whistler, both $C_{||}$ and C_e are essentially independent of β_e, but, for the kinetic Alfvén mode, $C_{||}$ increases with increasing β_e, whereas C_e shows the opposite trend. So as β_e increases the strong inequalities of Equations (4) and (5) are no longer valid.

Our kinetic theory results for $C_{\parallel}(k_{\perp})$ of the kinetic Alfvén wave are in qualitative agreement with the fluid model predictions of *Hollweg* [1999]. Even at $\beta_e = 2.0$, our calculations show $C_{\parallel} < C_{\perp\perp}$ into the short wavelength regime of strong Landau damping.

Consider the Maxwell equation $\nabla \cdot \delta\mathbf{B} = 0$ which implies $|\delta B_{\parallel}|^2 = \tan^2(\theta)|\delta B_y|^2$. Thus from Equation (2)

$$C_{\parallel} = (1 - C_{\perp\perp})\sin^2\theta$$

Note the $\sin^2(\theta)$ behavior of the magnetic compressibility in all three panels of Fig. 4 of *Saito et al.* [2008]. Calculations not shown here demonstrate that $C_{\perp\perp}$ is typically much closer to unity for kinetic Alfvén modes than for whistler fluctuations, from which Equation (4) follows.

3. Conclusions

We have used linear kinetic dispersion theory to compare some properties of quasi-perpendicular whistler and kinetic Alfvén fluctuatations at $\omega_p/c < k_{\perp} < \omega_e/c$. We show that at $\beta_e << 1$ the whistler in this regime is lightly damped over a broad range of quasi-perpendicular angles, $60^o < \theta < 90^o$, whereas the kinetic Alfvén fluctuations at such wavenumbers are lightly damped only for a very narrow cone of propagation, i.e., $89^o < \theta < 90^o$. We further find that such whistler fluctuations at $\beta_e << 1$ have relatively large magnetic compressibilities [defined by Equation (1)] and at sufficiently short wavelengths relatively small proton and electron compressibilities [defined by Equation (3)] as compared to kinetic Alfvén fluctuations.

If magnetic fluctuations are sufficiently weak, our linear theory results may be used to help discern the identity of the modes which contribute to dispersion range turbulence observed in the low-β the solar wind. ACE measurements of magnetic compressibility

in the high-frequency part of the inertial range show that $C_{\|}$ generally increases as both $|\delta\mathbf{B}|^2/B_o^2$ and β_p increase [*Smith et al.*, 2006b]. Recently this analysis has been extended to the dispersion range above the inertial range breakpoint; Fig. 8 of *Hamilton et al.* [2008] and Figure 7 of this manuscript demonstrate that the magnetic compressibility has the same qualitative response to β_p and $\delta B/B_o$ in the dispersion range as it does in the inertial range. Our theoretical result that magnetic compressibilities of kinetic Alfvén waves increase with plasma β is consistent with the interpretation that many of the points in Fig. 8 of *Hamilton et al.* [2008] are associated with that normal mode. On the other hand, the slope of the $C_{\|}$ versus β_p curve in the lower panel of Fig. 8 of *Hamilton et al.* [2008] is very shallow, suggesting that quasi-parallel whistlers (which have magnetic compressibilities which are small and relatively independent of β_e) may also contribute to the observations.

Furthermore, a number of data points from that figure and from Figure 7 correspond to $|\delta B_\perp|^2/|\delta B_\||^2 \leq 2$, that is, $C_{\|} \geq 1/3$. In particular, Fig. 8 of *Hamilton et al.* [2008] shows several observations of $C_{\|} \simeq 0.50$ at $\beta_p \lesssim 0.10$. Our theory has demonstrated that such large values of $C_{\|}$ at such low values of β cannot be generated by kinetic Alfvén waves, and so must correspond to quasi-perpendicular whistler fluctuations. We therefore conclude that some fraction of the observations of dispersion range turbulence in the solar wind are in the quasi-perpendicular whistler mode.

Our linear theory results indicate that the proton and electron compressibilities provide less clear-cut criteria for distinguishing between whistler and kinetic Alfvén modes; it requires both sufficiently small β_e and sufficiently large perpendicular wavenumbers to obtain Equation (5). Furthermore, the measurement cadence of spacecraft plasma instru-

ments is typically much slower than that of magnetometers, thereby precluding density measurements fast enough to **fully** address the high-frequency modes of the dispersion range.

At our present level of understanding, the best we can say is that quasi-parallel whistlers, quasi-perpendicular whistlers, and kinetic Alfvén waves all probably contribute to dispersion range turbulence in the solar wind. Thus the critical question is not which mode is present, but rather: What are the conditions which favor one mode over the others?

Acknowledgments.

The Los Alamos portion of this work was performed under the auspices of the U.S. Department of Energy (DOE). It was supported by the Magnetic Turbulence and Kinetic Dissipation Project of the Laboratory Directed Research and Development Program at Los Alamos, and by the Solar and Heliospheric Physics SR&T and the Heliophysics Guest Investigators Programs as well as by Cluster/PEACE data analysis funding of the National Aeronautics and Space Administration.

References

Alexandrova, O., V. Carbone, P. Veltri, and L. Sorriso-Valvo (2008), Small-scale energy cascade of the solar wind turbulence, *Astrophys. J., 674*, 1153.

Alexandrova, O., J. Saur, C. Lacombe, A. Mangeney, J. Mitchell, S. J. Schwartz, and P. Robert (2009), Universality of solar wind turbulent spectrum from MHD to electron scales, *Phys. Rev. Lett.,* **, in press.**

Bale, S. D., P. J. Kellogg, F. S. Mozer, T. S. Horbury, and H. Reme (2005), Measurement of the electric fluctuation spectrum of magnetohydrodynamic turbulence, *Phys. Rev.*

Lett., 94, 215002.

Beinroth, H. J., and F. M. Neubauer (1981), Properties of whistler mode waves between 0.3 and 1.0 AU from Helios observations, *J. Geophys. Res., 86*, 7755.

Biskamp, D., E. Schwarz, and J. F. Drake (1996), Two-dimensional electron magnetohydrodynamic turbulence, *Phys. Rev. Lett., 76*, 1264.

Biskamp, D., E. Schwarz, A. Zeiler, A. Celani, and J. F. Drake (1999), Electron magnetohydrodynamic turbulence, *Phys. Plasmas*, *6*, 751.

Cho, J., and A. Lazarian (2004), The anisotropy of electron magnetohydrodynamic turbulence, *Astrophys. J., 615*, L41.

Dasso, S., L. J. Milano, W. H. Matthaeus, and C. W. Smith (2005), Anisotropy in fast and slow solar wind fluctuations, *Astrophys. J., 635*, L181.

Dastgeer, S., A. Das, P. Kaw, and P. H. Diamond (2000), Whistlerization and anisotropy in two-dimensional electron magnetohydrodynamic turbulence, *Phys. Plasmas*, *7*, 571.

Galtier, S., and E. Buchlin (2007), Multiscale Hall-magnetohydrodynamic turbulence in the solar wind, *Astrophys. J., 656*, 560.

Gary, S. P. (1993), *Theory of Space Plasma Microinstabilities*, Cambridge Univ. Press, New York.

Gary, S. P., and J. E. Borovsky (2004), Alfvén-cyclotron fluctuations: Linear Vlasov theory, *J. Geophys. Res., 109*, A06105, doi:10.1029/2004JA010399.

Gary, S. P., and J. E. Borovsky (2008), Damping of long-wavelength kinetic Alfvén fluctuations: Linear theory, *J. Geophys. Res., 113*, A12104, doi:10.1029/2008JA013565.

Gary, S. P., S. Saito, and H. Li (2008), Cascade of whistler turbulence: Particle-in-cell simulations, *Geophys. Res. Lett., 35*, L02104, doi:10.1029/2007GL032327.

Gazis, P. R., and A. J. Lazarus (1982), Voyager observations of solar wind proton temperature: 1–10 AU, *Geophys. Res. Lett., 9*, 431.

Ghosh, S., E. Siregar, D. A. Roberts, and M. L. Goldstein (1996), Simulation of high-frequency solar wind power spectra using Hall magnetohydrodynamics, *J. Geophys. Res., 101*, 2493.

Goldstein, M. L., D. A. Roberts, and C. A. Fitch (1994), Properties of the fluctuating magnetic helicity in the inertial and dissipation ranges of solar wind turbulence, *J. Geophys. Res., 99*, 11,519.

Hamilton, K., C. W. Smith, B. J. Vasquez, and R. J. Leamon (2008), Anisotropies and helicities in the solar wind inertial and dissipation ranges at 1 AU, *J. Geophys. Res., 113*, A01106, doi:10.1029/2007JA012559.

Hollweg, J. V. (1999), Kinetic Alfvén wave revisited, *J. Geophys. Res., 104*, 14,811.

Horbury, T. S., M. A. Forman, and S. Oughton (2005), Spacecraft observations of solar wind turbulence: an overview, *Plasma Phys. Controlled Fusion*, *47*, B703.

Horbury, T. S., M. Forman, and S. Oughton (2008), Anisotropic scaling of magnetohydrodynamic turbulence, *Phys. Rev. Lett., 101*, 175005.

Howes, G. G. (2008), Inertial range turbulence in kinetic plasmas, *Phys. Plasmas*, *15*, 055904.

Howes, G. G., W. Dorland, S. C. Cowley, G. W. Hammett, E. Quataert, A. A. Schekochihin, and T. Tatsuno (2008a), Kinetic simulations of magnetized turbulence in astrophysical plasmas, *Phys. Rev. Lett., 100*, 065004.

Howes, G. G., S. C. Cowley, W. Dorland, G. W. Hammett, E. Quataert, A. A. Schekochihin, and T. Tatsuno (2008b), Reply, *Phys. Rev. Lett., 101*, 149502.

Leamon, R. J., C. W. Smith, N. F. Ness, W. H. Matthaeus, and H. K. Wong (1998), Observational constraints on the dynamics of the interplanetary magnetic field dissipation range, *J. Geophys. Res., 103*, 4775.

Leamon, R. J., W. H. Matthaeus, C. W. Smith, G. P. Zank, D. J. Mullan, and S. Oughton (2000), MID-driven kinetic dissipation in the solar wind and corona, *Astrophys. J., 537*, 1054.

Lengyel-Frey, D., R. A. Hess, R. J. MacDowall, R. G. Stone, N. Lin, A. Balogh, and R. Forsyth (1996), Ulysses observations of whistler waves at interplanetary shocks and in the solar wind, *J. Geophys. Res., 101*, 27,555.

Markovskii, S. A., B. J. Vasquez, and C. W. Smith (2008), Statistical analysis of the high-frequency spectral break of the solar wind turbulence at 1 AU, *Astrophys. J., 675*, 1576.

Matthaeus, W. H., M. L. Goldstein, and D. A. Roberts (1990), Evidence for the presence of quasi-two-dimensional nearly incompressible fluctuations in the solar wind, *J. Geophys. Res., 95*, 20,673.

Matthaeus, W. H., S. Servidio, and P. Dmitruk (2008), Comment on "Kinetic simulations of magnetized turbulence in astrophysical plasmas," *Phys. Rev. Lett., 101*, 149501.

Müller, W.-C., and R. Grappin (2005), Spectral energy dynamics in magnetohydrodynamic turbulence, *Phys. Rev. Lett., 95*, 114502.

Oughton, S., and W. H. Matthaeus (2005), Parallel and perpendicular cascades in solar wind turbulence, *Non. Proc. Geophys.*, *12*, 299.

Podesta, J. J. (2009), Dependence of solar-wind power spectra on the direction of the local mean magnetic field, *Astrophys. J., 698*, 986.

Sahraoui, F., M. L. Goldstein, P. Robert, and Yu. V. Khotyaintsev (2009), Evidence of a cascade and dissipation of solar-wind turbulence at the electron gyroscale, *Phys. Rev. Lett.,* **,** *102***, 231102.**

Saito, S., S. P. Gary, H. Li and Y. Narita (2008), Whistler turbulence: Particle-in-cell-simulations, *Phys. Plasmas*, *15*, 102305.

Schekochihin, A. A., S. C. Cowley, W. Dorland, G. W. Hammett, G. G. Howes, E. Quataert, and T. Tatsuno (2009), Astrophysical gyrokinetics: Kinetic and fluid turbulenct cascades in magnetized weakly collisional plasmas, *Astrophys. J. Suppl. Series*, *182*, 310.

Shaikh, D., and P. K. Shukla (2009), 3D simulations of fluctuation spectra in the Hall-MHD plasma, *Phys. Rev. Lett., 102*, 045004.

Smith, C. W., D. J. Mullan, N. F. Ness, R. M. Skoug, and J. Steinberg, (2001), Day the solar wind almost disappeared: Magnetic field fluctuations wave refraction and dissipation, *J. Geophys. Res., 106*, 18,625.

Smith, C. W., K. Hamilton, B. J. Vasquez, and R. J. Leamon (2006a), Dependence of the dissipation range spectrum of interplanetary magnetic fluctuations on the rate of energy cascade, *Astrophys. J., 645*, L85.

Smith, C. W., B. J. Vasquez, and K. Hamilton (2006b), Interplanetary magnetic fluctuation anisotropy in the inertial range, *J. Geophys. Res., 111*, A09111, doi:10/1029/2006JA011651.

Stawicki, O., S. P. Gary, and H. Li (2001), Solar wind magnetic fluctuation spectra: Dispersion versus damping, *J. Geophys. Res., 106*, 8273.

328 Tessein, J. A., C. W. Smith, B. T. MacBride, W. H. Matthaeus, M. A. Forman, and J. E.
329 Borovsky (2009), Spectral indices for multi-dimensional interplanetary turbulence at 1
330 AU, *Astrophys. J., 692*, 684.
331 Wareing, C. J., and R. Hollerbach (2009), Forward and inverse cascades in decaying two-
332 dimensional electron magnetohydrodynamic turbulence, *Phys. Plasmas*, *16*, 042307.

Figure 1. The real frequencies (solid and dashed lines) and damping rates (dotted lines) of whistler fluctuations as functions of $k_\perp c/\omega_e$ for three different values of θ as labeled. Here $\beta_e = 0.10$ and $T_e/T_p = 1.0$.

Figure 2. The real frequencies (solid and dashed lines) and damping rates (dotted lines) of kinetic Alfvén fluctuations as functions of $k_\perp c/\omega_p$ for three different values of θ as labeled. Here $\beta_p = 0.10$ and $T_e/T_p = 1.0$.

Figure 3. The electron compressibility (solid and dashed lines) and magnetic compressibility (dotted lines) of whistler fluctuations as functions of $k_\perp c/\omega_e$ for the same three cases shown in Figure 1.

Figure 4. The electron compressibility (solid and dashed lines) and magnetic compressibility (dotted lines) of kinetic Alfvén fluctuations as functions of $k_\perp c/\omega_p$ for the same three cases shown in Figure 2.

Figure 5. The magnetic compressibility (dotted lines) and electron compressibility (solid and dashed lines) of whistler fluctuations as functions of $k_\perp c/\omega_e$ at $\theta = 80^o$ for two different values of β_e as labeled. At this angle of propagation and $\beta_e = 2.0$, the whistler is generally heavily damped and is not shown here.

Figure 6. The magnetic compressibility (dotted lines) and electron compressibility (solid and dashed lines) of kinetic Alfvén fluctuations as functions of $k_\perp c/\omega_p$ at $\theta = 80^o$ for three different values of β_e as labeled.

Figure 7. Scatterplot of magnetic field anisotropy versus $\delta B/B_o$ using solar wind observations from the ACE spacecraft. Red (black) points represent cloud (open) magnetic field lines. (a) Measurements corresponding to the inertial range [Fig. 4 from *Smith et al.*, 2006b]. (b) Measurements from the dispersion range.

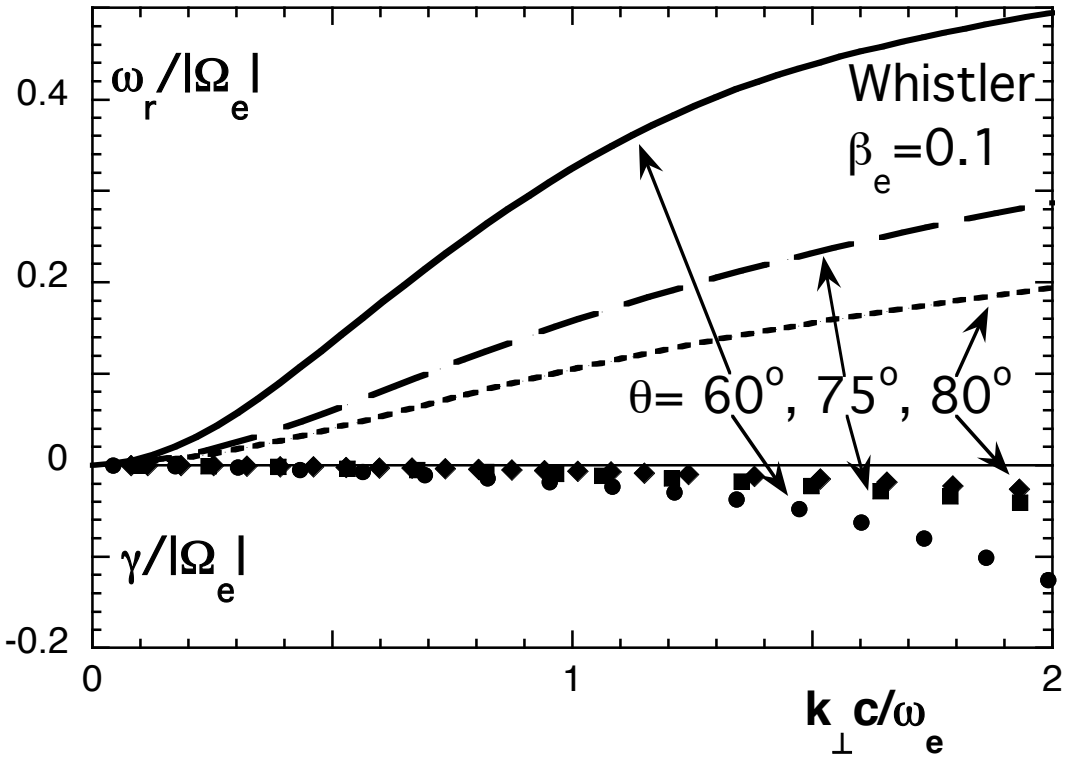

Figure 1

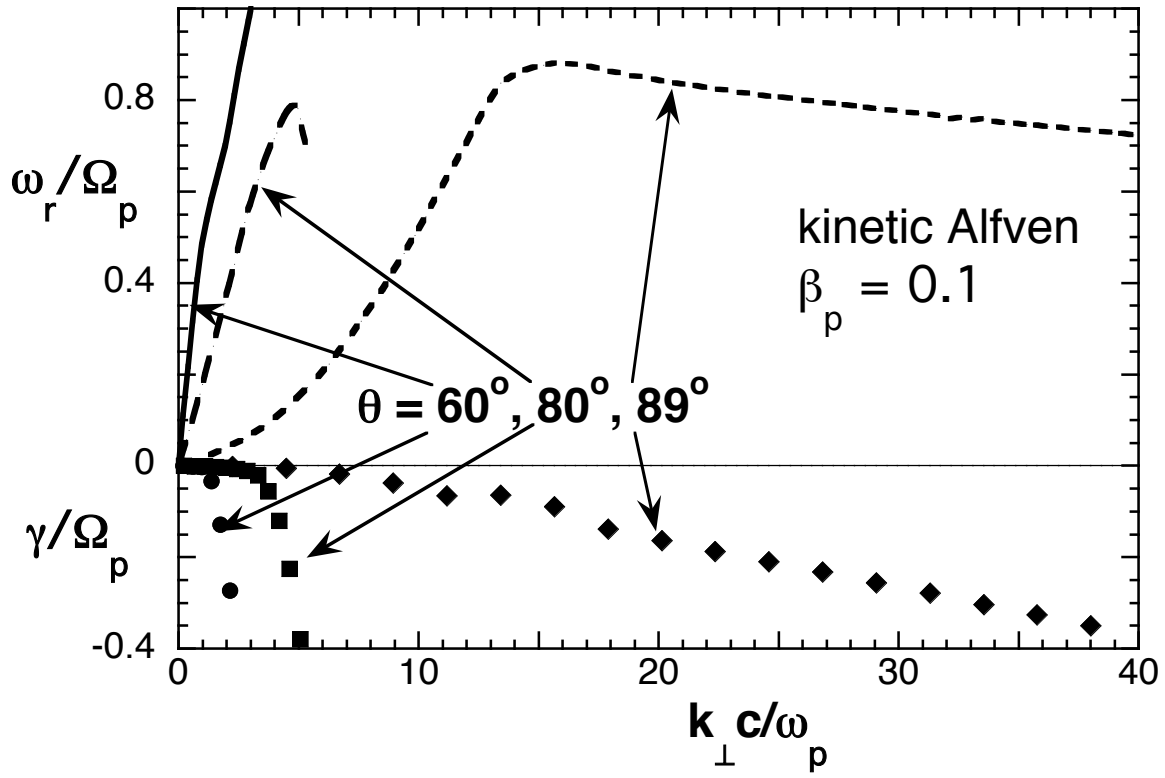
0.8
0.4
0
-0.4
ω_r/Ω_p
γ/Ω_p
kinetic Alfven
β_p = 0.1
θ = 60°, 80°, 89°
0
10
20
30
40
k_⊥ c/ω_p

Figure 2

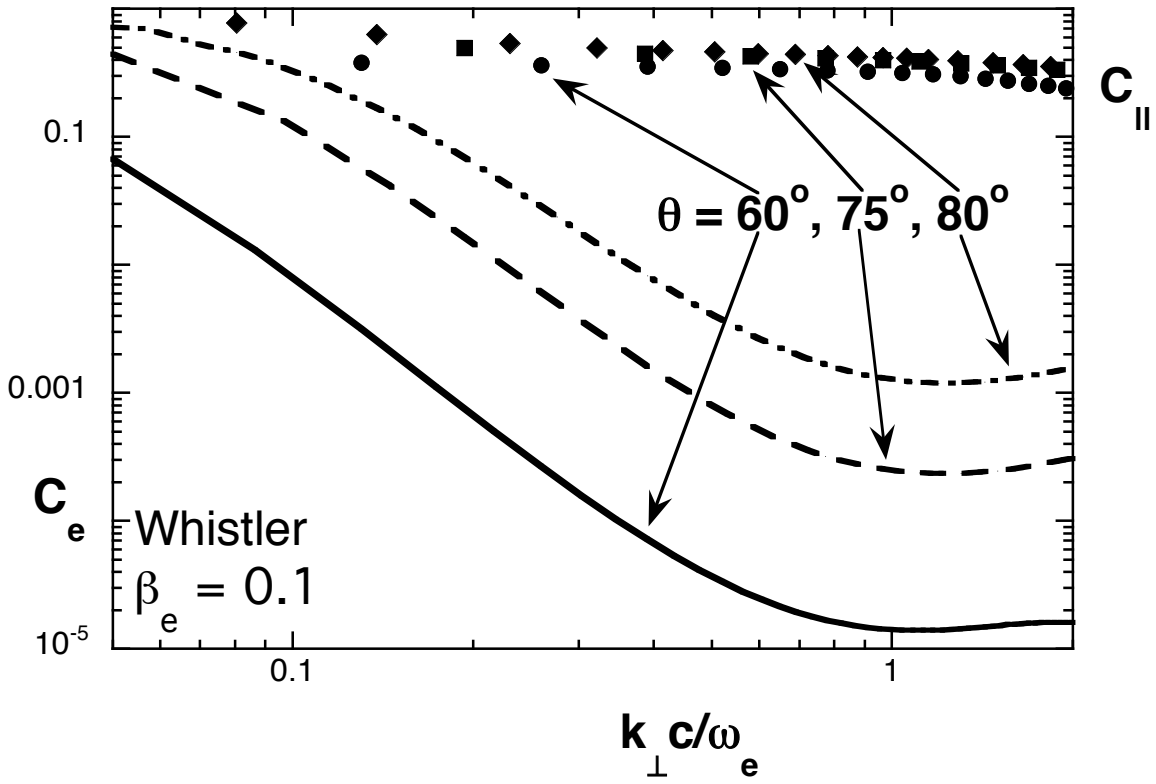
0.1
0.001
10^{-5}
C_e
Whistler
$\beta_e = 0.1$
0.1
1
$k_\perp c/\omega_e$
C_{II}
$\theta = 60^o, 75^o, 80^o$

Figure 3

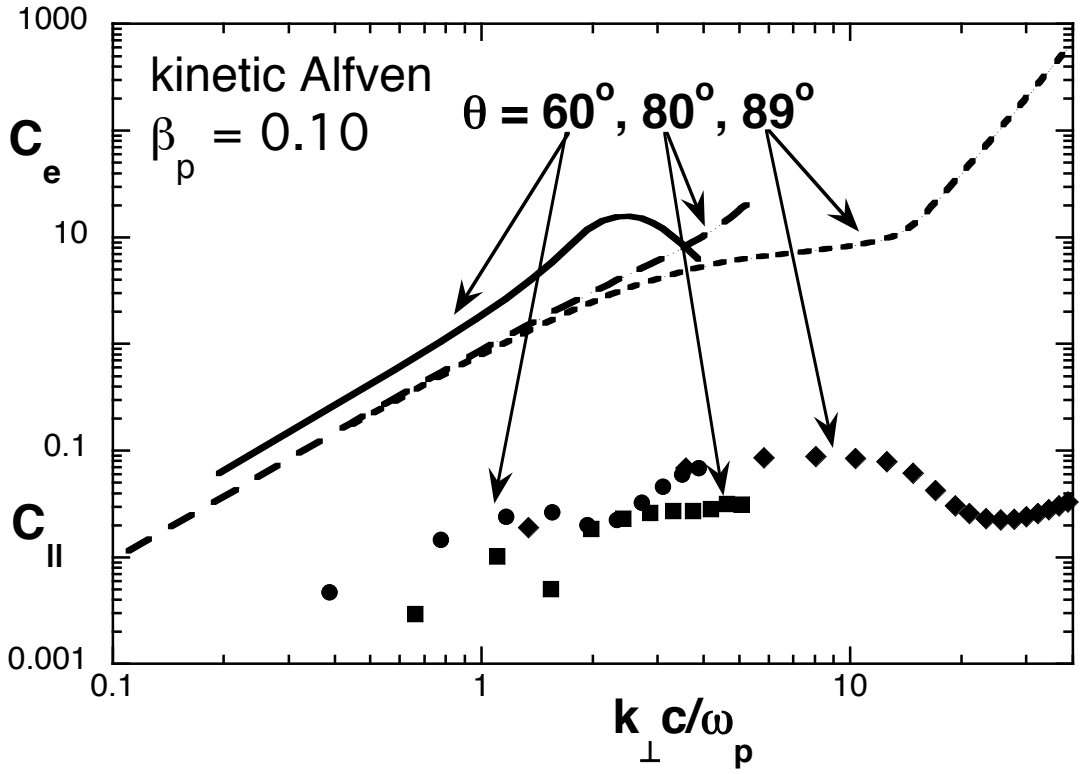
kinetic Alfven
β_p = 0.10
θ = 60°, 80°, 89°
C_e
C_{II}
1000
10
0.1
0.001
0.1
1
10
$k_\perp c/\omega_p$

Figure 4

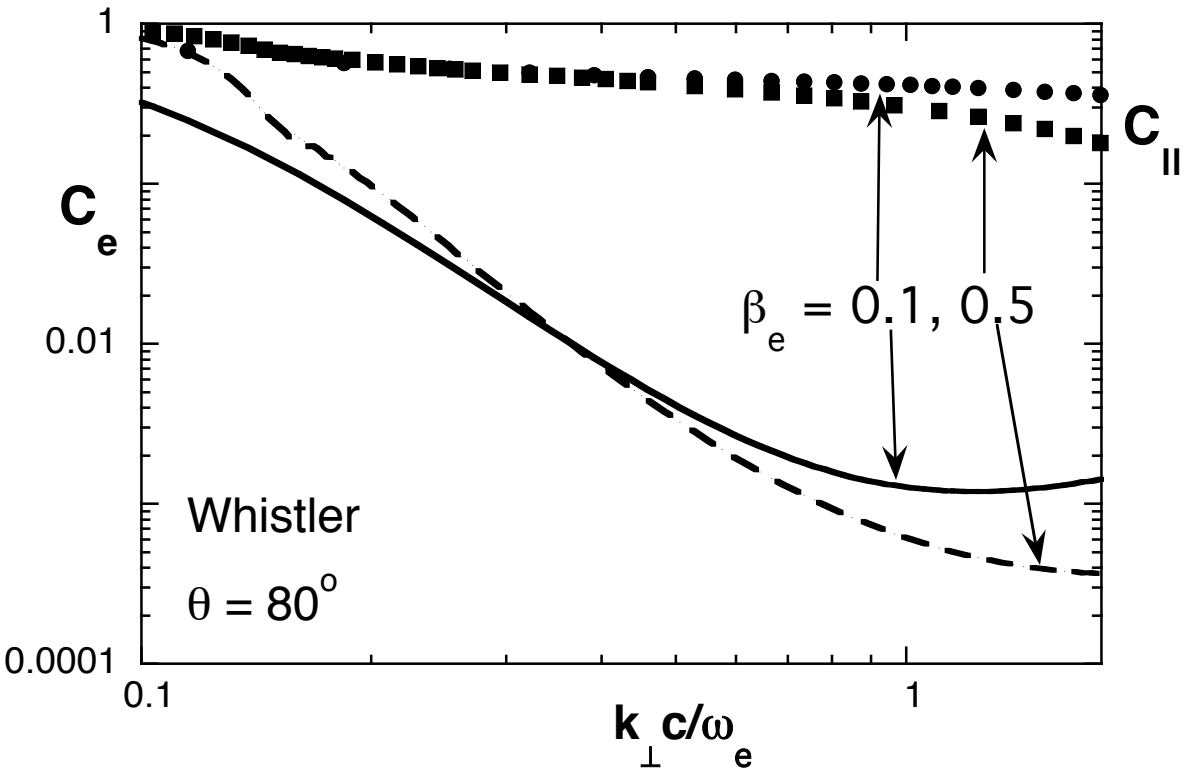

Figure 5

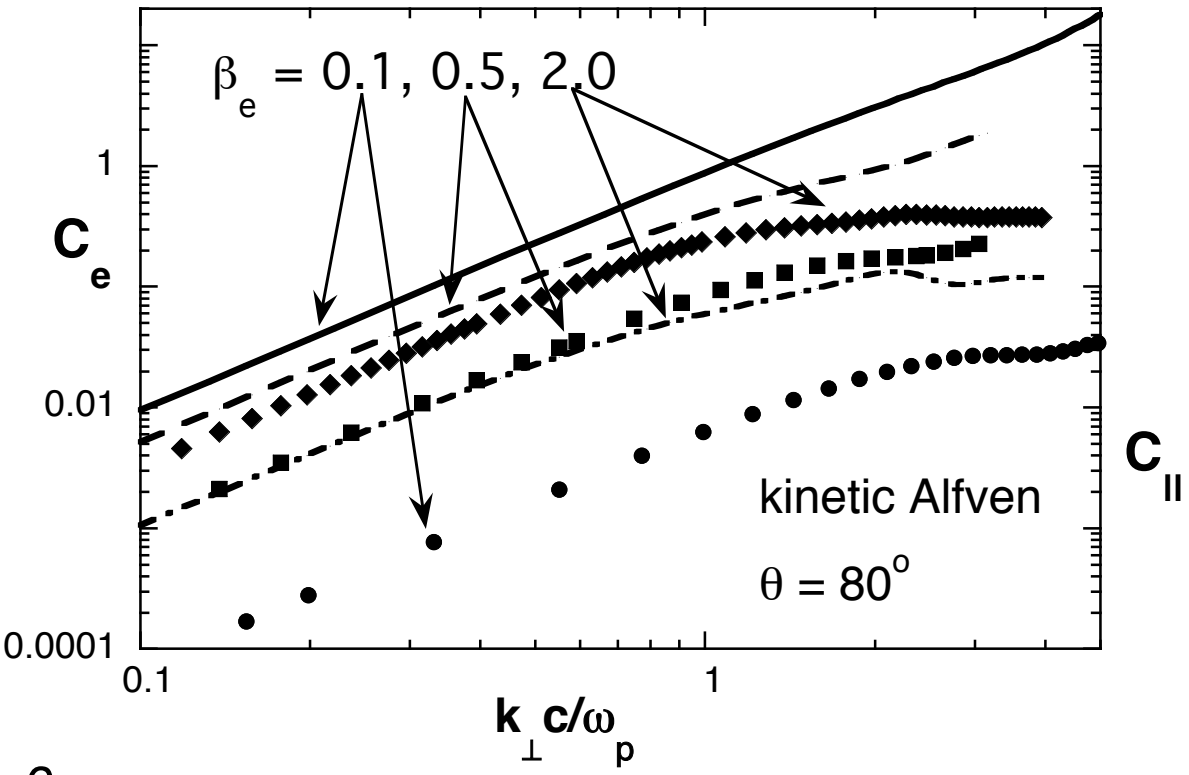
β_e = 0.1, 0.5, 2.0
1
0.01
0.0001
C_e
0.1
1
$k_\perp c/\omega_p$
kinetic Alfven
$\theta = 80^o$
C_{II}

Figure 6

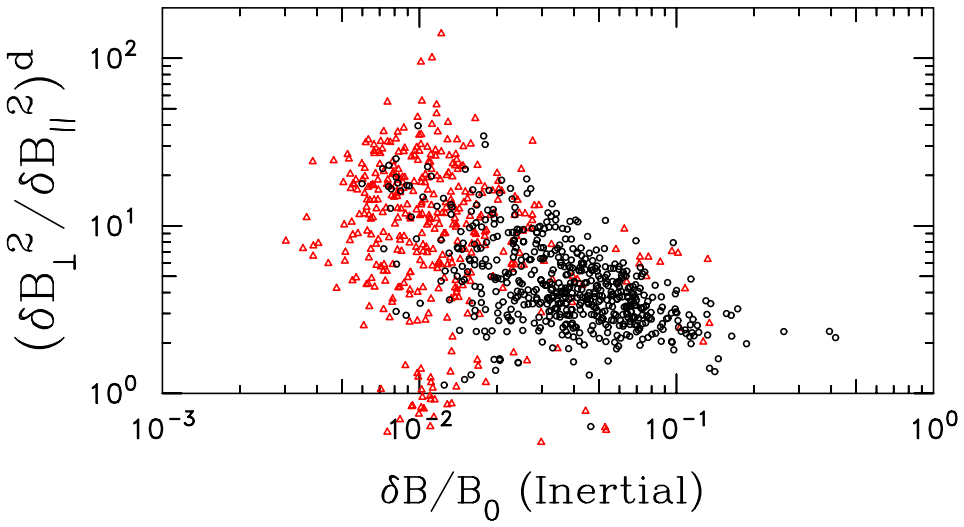
$(\delta B_\perp^2/\delta B_{||}^2)^d$
10^2
10^1
10^0
10^{-3}
10^{-2}
10^{-1}
10^0
$\delta B/B_0$ (Inertial)

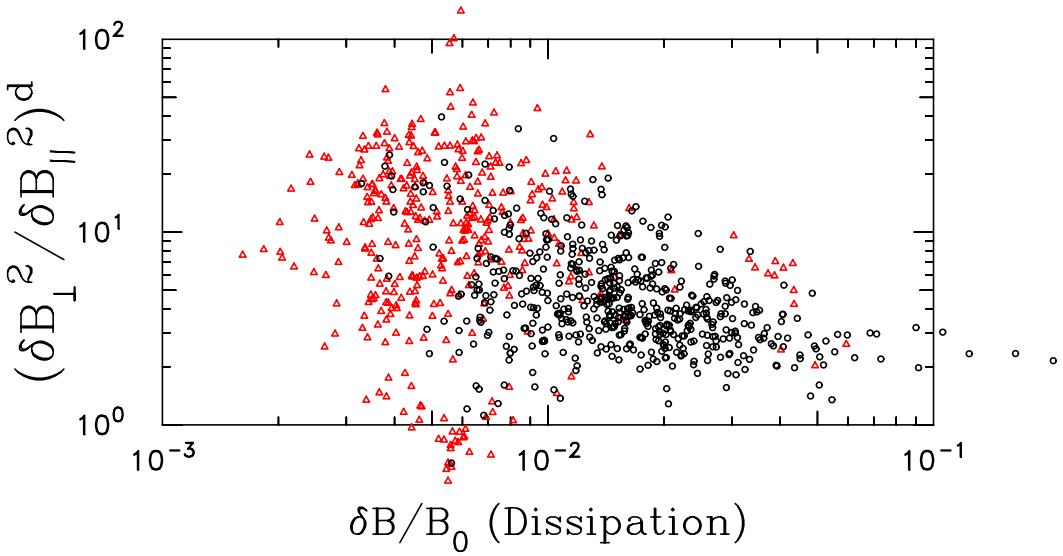
$(\delta B_\perp^2/\delta B_{||}^2)^d$
10^2
10^1
10^0
10^{-3}
10^{-2}
10^{-1}
$\delta B/B_0$ (Dissipation)